Langmuir

Invited Feature Article

pubs.acs.org/Langmuir

Lateral Intermolecular Self-Exchange Reactions for Hole and Energy Transport on Mesoporous Metal Oxide Thin Films

Ke Hu and Gerald J. Meyer*

Department of Chemistry, University of North Carolina at Chapel Hill, Chapel Hill, North Carolina 27599, United States

ABSTRACT: Intermolecular self-exchange energy and electron-transfer reactions occur without a loss of free energy. This behavior can be exploited for energy-transport applications when molecules that undergo self-exchange transfer reactions are immobilized on a solid support. This Article focuses upon lateral self-exchange reactions and the relevant interfacial chemistry that occurs on the mesoporous nanocrystalline (anatase) TiO_2 thin films that are commonly used in dye-sensitized solar cells. It has been known for some time that all of the dye molecules (termed sensitizers) within such thin films can be reversibly oxidized and reduced by lateral self-exchange electron transfer provided that the sensitizer surface coverage exceeds a percolation threshold. Under conditions where excited-state electron injection into TiO_2 is unfavored, lateral intermolecular energy-transfer reactions are also known to occur. The self-exchange rate constants have been quantified by electrochemical, absorption, and/or time-resolved anisotropy techniques and understood within the framework of Marcus theory. Such analysis reveals that the reorganization energy and the electronic coupling are sensitive to the identity of the molecular compound. Time-resolved anisotropy measurements have shown that lateral charge and energy-transfer reactions across the TiO_2 surface occur in kinetic competition with charge recombination and excited-state relaxation, respectively. The extent to which lateral self-exchange reactions might be exploited for solar energy conversion applications is discussed, as are critical fundamental issues that remain unresolved.

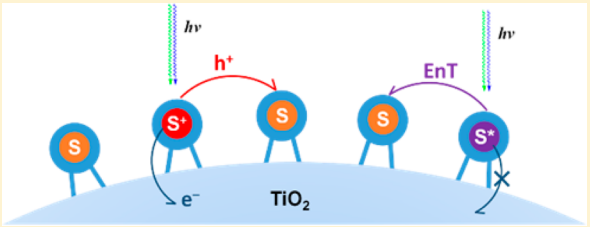

I. INTRODUCTION

Materials that transport charge or excited-state energy without a loss in the Gibbs free energy are of considerable interest to the growing scientific community that hope to identify practically useful materials for solar energy conversion. Self-exchange reactions transfer charge or excited-state energy from one compound to another and yield products that are equivalent to the reactants, hence $\Delta G^{o} = 0$ for reactions 1 and 2.[1−3]

$$Ru(bpy)_3^{3+} + Ru(bpy)_3^{2+} \rightarrow Ru(bpy)_3^{2+} + Ru(bpy)_3^{3+} \quad (1)$$

$$Ru(bpy)_3^{2+*} + Ru(bpy)_3^{2+} \rightarrow Ru(bpy)_3^{2+} + Ru(bpy)_3^{2+*} \quad (2)$$

When related compounds have been linked to a solid oxide surface, the corresponding self-exchange transfer reactions provide a molecular basis for the transport of electrons, holes, or excited-state energy laterally across the surface without free-energy losses. For example, it was recently shown that after excited-state dye-sensitized electron injection into TiO_2 the oxidized dye that is formed "hops" away from the injection site to neighboring dye molecules by self-exchange electron-transfer reactions commonly referred to as "hole hopping" (Figure 1A).[4,5] When excited-state injection into TiO_2 is unfavored, the excited state can instead transfer energy to a neighboring sensitizer providing a basis for energy transport (Figure 1B).[6,7] While clear precedence for both reactions has been available for some time, the full extent to which they can be exploited for solar energy conversion remains unclear. What we think we know, what we do not know, and what we would like to know about such self-exchange reactions and the interfacial molecular oxide chemistry relevant to them are the focus of this Invited Feature Article.

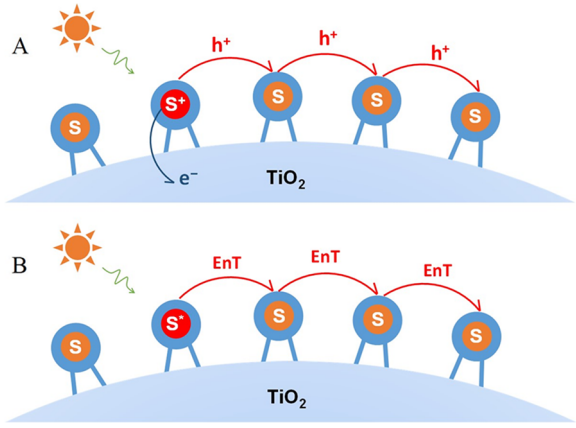

Figure 1. (A) Excited-state electron injection by a sensitizer followed by $S^{+/0}$ self-exchange hole hopping and (B) excited-state $S^{*/0}$ energy transfer across the TiO_2 surface.

Received: June 10, 2015
Revised: July 29, 2015
Published: July 29, 2015

DOI: 10.1021/acs.langmuir.5b02129
Langmuir 2015, 31, 11164−11178

Self-exchange electron-transfer reactions such as that given in eq 1 are now understood in considerable detail in homogeneous fluid solution. Marcus theory for electron transfer has been successfully utilized to quantify self-exchange data and to predict the rate constants for cross-reactions that involve a chemical and free-energy change.[8] The expressions derived by Marcus are expressed in terms of energies rather than free energies; however, this is not an issue for self-exchange reactions because ΔS^{o} (and ΔG^{o}) are equal to zero. A simplified one-dimensional diagram for a self-exchange reaction is given in Figure 2. The self-exchange rate constant, k_{se}, is

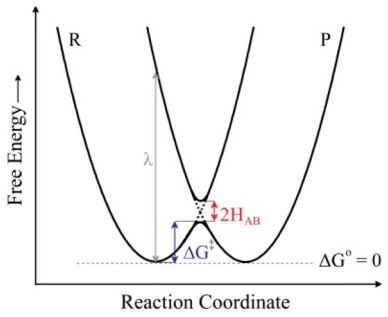

Figure 2. One-dimensional free-energy surfaces for adiabatic (solid lines) and nonadiabatic (dashed lines) self-exchange electrons or energy transfer. The reorganization energy, λ, and the donor–acceptor electronic coupling, H_{AB}, are indicated. The Gibbs free energy change for the reaction is zero as the reactant R and product P are equivalent.

dependent upon the temperature (T), the reorganization energy (λ), and the donor–acceptor electronic coupling (H_{AB}) (eq 3).

$$k_{se} = \frac{2\pi}{\hbar}|H_{AB}|^2 \frac{1}{\sqrt{4\pi\lambda k_b T}} \exp\left(-\frac{\lambda}{4k_b T}\right) \quad (3)$$

Immobilization on an oxide surface would be expected to restrict molecular motions and the formation of the "encounter complex" that precedes electron transfer in fluid solution. Hence nonadiabatic electron transfer with even weaker electronic coupling is expected for electron self-exchange of molecules immobilized and site isolated on oxide surfaces, $H_{AB} \ll kT$.[9] Adiabatic pathways may become operative under conditions when the molecules aggregate.[10] One would also anticipate that H_{AB} could be controlled experimentally and systematically by varying the surface coverage and hence the intermolecular distance R over which self-exchange occurs. While some evidence for this exists,[11] systematic studies that would enable the determination of a damping factor β are unavailable; $H_{AB} = H_{ABo}\exp[-\beta(R - R_o)]$, where H_{ABo} is the electronic coupling at van der Waals separation R_o. Almost all studies to date have been performed at saturation surface coverages where the sensitizers are generally assumed to be in van der Waals contact.

The semiconducting nature of an oxide such as TiO_2 could enhance H_{AB} relative to sensitizers anchored to an insulating oxide support, such as Al_2O_3 or ZrO_2. Comparative studies of this type reveal that hole hopping is not grossly different yet is not exactly the same, behavior that may result from the experimental challenge of preparing mesoporous thin films of different oxide materials that enable meaningful comparisons or an indication that the oxide itself can mediate hole hopping.[11,12] It is simply unknown for mesoporous oxide materials that are insulating in the dark. For highly doped intrinsic oxide materials that are utilized as transparent conductive oxides (TCOs), such as fluorine-doped tin oxide (FTO), there is no question that the oxide itself can mediate electron transfer. Under conditions of forward bias (negative applied potentials), TiO_2 becomes more highly conductive and may indeed mediate self-exchange reactions.[13] However, most hole-hopping studies to date have not been performed under such conditions. Indeed the state-of-the-art data for hole hopping in mesoporous TiO_2 nanocrystalline (anatase, 10–20 nm diameter) thin films is completely consistent with the conclusion that the S and S^+ charges (or S* for energy transfer) remain confined within the molecular frontier orbitals of the sensitizer.[14] Testing this conclusion and developing a better understanding of how doping and oxide conductivity influence hole hopping represent areas ripe for future research.

The normal partitioning of the reorganization energy as a sum of inner- and outer-sphere contributions, $\lambda = \lambda_i + \lambda_o$, requires further evaluation when sensitizers are anchored to oxide surfaces. The surface atoms that interact with the sensitizer could be viewed as part of the inner molecular sphere (λ_i) or the outer sphere (λ_o). The asymmetry of the sensitizer–TiO_2 interface also complicates the evaluation of λ_o. The sensitizer may be partially "solvated" by surface titanol groups, water, and adsorbed surface ions as well as the external solvent/electrolyte present in the mesopores. A recent study constrained λ_i to include only the sensitizer;[15] everything else was considered part of the outer sphere. Interestingly, these same authors concluded that both H_{AB} and λ for lateral hole hopping were dependent upon the orientation of the frontier orbitals and the chemical nature of the sensitizers.[15]

In this Feature Article, lateral intermolecular charge- and energy-transfer self-exchange reactions that occur within the mesoporous nanocrystalline (anatase) TiO_2 thin films commonly used in dye-sensitized solar cells (DSSCs) are highlighted. The Article is not meant to be an exhaustive review but rather to provide an introduction to the field with some illustrative examples that demonstrate their potential utility in solar energy conversion and the need for continued fundamental study. As the invitation from *Langmuir* demands, the Article is focused mainly upon research from our own laboratories; however, considerable effort was made to appropriately cite the relevant literature. We begin with the early observations that led researchers to conclude that lateral self-exchange reactions were indeed occurring on the TiO_2 surface along with some speculation about the interfacial chemistry. A detailed summary of the current state of the art in this field that reveals new directions for future research follows. We conclude with unanswered questions important for fundamental and applied research.

II. EARLY EVIDENCE FOR SELF-EXCHANGE ENERGY AND ELECTRON TRANSFER IN MESOPOROUS TIO_2

Interfacial Chemistry. Our research at Johns Hopkins University began in 1991, the same year that a key paper appeared reporting the sol–gel synthesis of mesoporous TiO_2 nanocrystalline (anatase, 10–20 nm diameter) thin films (5–10 μm) for solar energy conversion applications.[16] This sol–gel chemistry differed from previous synthetic approaches in that the titanium alkoxide hydrolysis and polycondensation reactions were completed in fluid solution before (rather than after) deposition on fluorine-doped tin oxide (FTO) conductive substrates.[17] The preparation of a colloidal solution

DOI: 10.1021/acs.langmuir.5b02129
Langmuir 2015, 31, 11164–11178

that could later be deposited onto conductive substrates provided reproducible mesoporous thin films with high transparency in the visible and near-IR regions. Closely related materials are now commercially available.

The TiO_2 thin films were sensitized to visible light with Ru(II) polypyridyl compounds that possess carboxylic acid functional groups. A sensitizer that has been studied in considerable detail is $[Ru(bpy)_2(dcb)]^{2+}$, where dcb is 4,4′-$(CO_2H)_2$-2,2′-bipyridine. The surface functionalization is performed at room temperature in organic solvents, most commonly CH_3CN or CH_3CH_2OH. Goodenough first proposed that a dehydrative coupling reaction between the carboxylic acid groups and surface titanol groups yields surface ester linkages (Figure 3).[18] It is worthwhile yet very humbling to reflect upon what truly is known about this surface chemistry and the molecular nature of the sensitized interface.

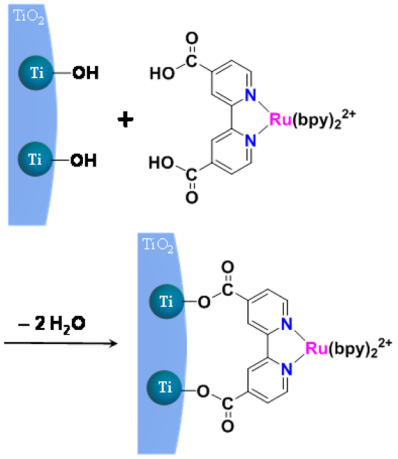

Figure 3. Goodenough's proposed dehydrative surface reaction for anchoring a ruthenium sensitizer with a dcb (4,4′-$(CO_2H)_2$-2,2′-bipyridine) ligand to TiO_2. Adapted with permission from ref 18. Copyright 1979 Nature Publishing Group.

The identity of the surface linkage has been revealed most successfully by attenuated total reflection infrared spectroscopy (ATR-FTIR).[19,20] Raman experiments performed in resonance with the Ru → dcb MLCT absorption have failed to show enhancements of the carboxylate groups, presumably because they are orthogonal to the π system of the pyridine ring.[21] Early FTIR studies of Degussa P-25[22] and acid-pretreated TiO_2[14] revealed an asymmetric CO stretch at 1730 cm^{-1} attributed to the presence of surface ester linkages or simply unreacted carboxylic acids. In addition, a broad and more intense band was observed at 1603 cm^{-1}, consistent with a C−O bond order of 1.5 and the presence of carboxylate groups. It is clear from many studies that carboxylate binding is the operative motif with the DSSC processing conditions used today. The fate of the carboxylic acid proton remains uncertain. In principle, the energy separation between the symmetric and asymmetric C−O stretches can provide more detailed information on the exact nature of carboxylate coordination;[23] however, at TiO_2 interfaces it is not even possible to conclude confidently that the carboxylates are coordinated to Ti metal centers.[21] Indeed the ATR-FTIR spectrum of the sensitizer is often found to be insensitive to the identity of the oxide material. The translational mobility and fluxionality of sensitizers anchored to TiO_2 through carboxylates or other surface linkages remain largely unknown and require more detailed study that is of particular importance to understanding the self-exchange reactivity. The observation of a percolation threshold and anisotropy responses described below indicate that the sensitizers do not reorient on a 10^{-9} to 10^{1} s time scale under some specific conditions.

Goodenough did not consider the surface functionalization chemistry to be reversible. However, adsorption isotherm data reported since for $Ru(bpy)_2(dcb)$ /TiO_2 and related Ru(II) compounds clearly demonstrated that the surface coverage reached a limiting value when the solution concentration was $\geq 3 \times 10^{-4}$ M.[21,24−26] Fits to the Langmuir adsorption isotherm model provided estimates of the equilibrium constants that ranged from $K_{eq} = 10^5$ to 10^6 M^{-1} with saturation surface coverages of 2×10^{-8}–8×10^{-8} mol/cm^2. These coverages are often asserted to correspond to that of a molecular monolayer; however, such an assertion is difficult to prove experimentally since the oxide surface area available to sensitizers is poorly defined within these mesoporous thin films. Although the sensitizer aggregation has been very well documented for neutral organic dye molecules such as coumarins,[27] there has been vanishingly little spectroscopic evidence for this with Ru polypyridyl sensitizers. We therefore speculate that $[Ru(bpy)_2(dcb)]^{2+}$ (and other Ru(II) sensitizers) are present on TiO_2 in a monolayer or lower surface coverages. The average number of Ru compounds on each anatase nanocrystallite can be estimated through Beer's law and gravimetric analysis of the mesoporous thin films, typically providing values of about 400 ± 200 sensitizers per nanocrystallite with variations in porosity and shape of the nanoparticles.[28,29] Even with such a large uncertainty, establishing the approximate stoichiometry is useful in developing molecular-level descriptions of the interface.

A curious aspect of the equilibrium binding was discovered very early on. When sensitized thin films were placed back in neat CH_3CN, little to no surface desorption occurred over periods of days. Such behavior was inconsistent with the envisioned dynamic equilibrium implied by good fits of the isotherm data to the Langmuir model. Our rationalization at the time was that an initial equilibrium was established between the protonated form of the sensitizer and the surface followed by subsequent acid−base chemistry that yielded the carboxylate form of the sensitizers. We now suspect that the entire interface may reconstruct after sensitizer functionalization. The analogous reactions with mesoporous ZnO thin films are known to yield soluble Zn(II) carboxylate compounds,[30] and it is reasonable to believe that the less labile Ti(IV) ions remain associated with the bulk solid. Studies where the TiO_2 was pretreated with aqueous acid or base solution prior to characterization in organic solvents, suggested the presence of a hydrated surface layer wherein the TiO_2 acceptor states could be tuned in energy[14] much like the conduction band edge of single-crystal rutile TiO_2 in aqueous solution.[31] In addition, a recently discovered electroabsorption signature induced by electrons injected into TiO_2 has provided new insights into the dynamics of ion exchange at the interface that are most consistent with cations inserting themselves between the sensitizer and the crystalline TiO_2.[32,33] Taken together, this data suggests the presence of a hydrated soft gel-like layer between the molecular sensitizers from the hard ceramic bulk.

In summary, there exists precious little direct information on the molecular nature of sensitizer−TiO_2 interfaces, but there is growing, albeit indirect, evidence of an amorphous layer where ions and solvent molecules can rapidly reorganize in response

DOI: 10.1021/acs.langmuir.5b02129
Langmuir 2015, 31, 11164−11178

to external stimuli such as changes in the light intensity, applied potential, or electrolyte composition. Therefore, although Goodenough's proposed surface chemistry and idealized "cartoons" (such as that shown in Figure 3) imply a sharp and well-defined TiO_2–molecule interface, this may in fact convey the wrong conceptual image. New in situ analytical techniques that provide direct structural information on the molecular interface are critically needed.

Electron Self-Exchange. In 1996, sensitized Ru-$(dmb)_2(LL)/TiO_2$ films, where dmb is 4,4′-$(CH_3)_2$-2,2′-bipyridine and LL is 4-(CH_3)-4′-(COOH)-2,2′-bipyridine, 4-(CH_3)-4′-$((CH_2)_3$COOH)-2,2′-bipyridine, or 4-(CH_3)-4′-$((CH_2)_3$-$COCH_2COOC_2H_5)$-2,2′-bipyridine (bpy-acac), were employed as the working electrodes in standard three-electrode electrochemical cells. Surprisingly, quasi-reversible waves were observed in cyclic voltammograms that were reasonably assigned to the $Ru^{III/II}$ reductions.[24] The electroactive surface coverage at moderate 20–200 mV/s scan rates were at least a factor of 10 larger than what could reasonably be attributed to sensitizers anchored to the conductive FTO substrate. The measured $Ru^{III/II}$ reduction potentials were energetically within the forbidden band gap of TiO_2. Taken together, these observations suggested that the high electroactive surface coverages resulted from electron transfer initiated at the FTO substrate that continued across the nanocrystalline TiO_2 surface(s) by lateral self-exchange hole hopping. At the scan rates employed only about 10% of the sensitizers were oxidized.

Quite independent of our own efforts, a landmark paper in this area was reported by Bonhôte and co-workers in 1998.[11] Remarkably, these scientists showed that within reasonable experimental error all of the triaryl amine sensitizers within a mesoporous TiO_2 thin film could be reversibly oxidized within a few seconds after an applied potential step provided that the sensitizer surface coverage exceeded a percolation threshold of about 50% of the saturation value. Such a three-dimensional percolation model is shown in Figure 4 for the first few

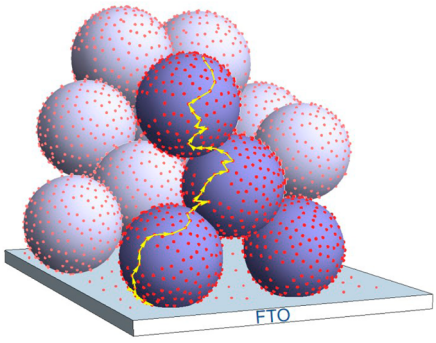

Figure 4. Charge percolation from the FTO substrate across the surface of nanocrystalline oxide materials (light- and dark-blue spheres) that comprise a mesoporous thin film. The red dots represent surface-anchored sensitizer molecules. The yellow arrows show one possible charge percolation pathway from the FTO substrate to sensitizers at the top of the thin film.

sensitized ~20-nm-diameter TiO_2 nanocrystals on an FTO substrate. The nanocrystals were sensitized to approximately half the saturation surface coverage. The yellow arrows indicate a hole-hopping percolation pathway from the FTO up though the thin film. Note that the number of nearest-neighbor hopping pathways was limited, demonstrating that the surface coverage was just above the percolation threshold. At higher surface coverages, additional pathways become operative.

Measurements in different electrolytes and as a function of surface coverage revealed that self-exchange was dependent on both the electron-transfer rate and the density of conducting paths. Similar redox behavior was observed with insulating Al_2O_3 nanoparticles providing evidence that the oxide band structure was not an important variable for the self-exchange reactions. These self-exchange reactions were quantified by spectroelectrochemistry. Upon application of a potential step, the color change that accompanied the sensitizer redox chemistry was monitored spectroscopically on millisecond time scales. An apparent diffusion rate constant D_{app}, was abstracted from analysis with the Cottrell equation (eq 4),

$$\Delta A = \frac{2\Delta A_f D_{app}^{0.5} t^{0.5}}{d\pi^{0.5}} \quad (4)$$

where ΔA is the time-dependent absorbance change, ΔA_f is the final absorbance change, and d is the film thickness. As is often done today, the absorption (or current) change measured after a potential step is plotted versus the square root of time in an Anson plot. A typical Anson plot is shown in Figure 5. D_{app} is

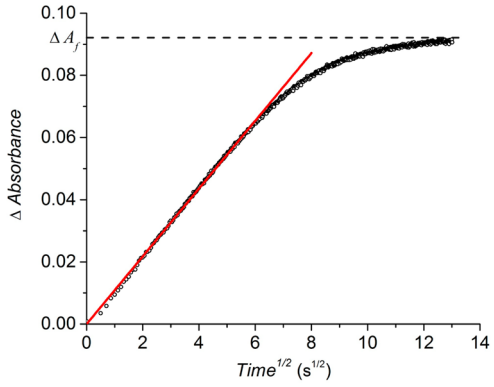

Figure 5. Typical Anson plot of the potential induced absorption change as a function of the square root of time. The red line is a linear fit to the initial absorption change. The dashed black line indicates the final absorbance change that reaches a steady state value.

abstracted from the slope of the initial linear region. Bonhote and others since have found that it is generally possible to fit more than two-thirds of the measured ΔA vs $t^{1/2}$ plot for mesoporous TiO_2 thin films, although this likely depends upon experimental details. As eq 4 is based upon a semi-infinite diffusion boundary approximation and the mesoporous thin film has a finite thickness, this model is valid only until the "front" of oxidized molecules approaches the outer edge of the thin film, after which time all of the sensitizers are completely oxidized and the absorption change becomes time-independent.

The D_{app} values have been directly related to the first-order self-exchange rate constants, k_{hop}, and the second-order rate constant, k_{se}, with eq 5, where δ is the equilibrium intermolecular separation and hence the effective length of the hop between sensitizers in the mesoporous thin film.[34,35]

$$D_{app} = \frac{k_{hop}\delta^2}{6} = \frac{k_{se}C\delta^2}{6} \quad (5)$$

Concentration C within the mesoporous thin films is ill-defined as the sensitizers are surface confined on the TiO_2 nano-

DOI: 10.1021/acs.langmuir.5b02129
Langmuir 2015, 31, 11164–11178

particles. The number of moles of redox-active sensitizers can be determined experimentally through visible absorption or coulometry measurements; however, the volume occupied is uncertain due to the mesoporous structure of the thin film. Some experimentalists utilize the entire volume of the thin film to calculate an approximate concentration, and although these values are of debatable use, they do enable comparisons with solution self-exchange data that are typically reported in units of M^{-1} s^{-1}.[11]

Energy Self-Exchange. We were initially surprised to find that visible light illumination of a $Ru(bpy)_2(dcb)/TiO_2$ thin film immersed in neat CH_3CN resulted in intense photoluminescence (PL) from long-lived metal-to-ligand charge transfer (MLCT) excited states.[36] Ultrafast excited-state injection was well documented and expected in the late 1990s[37] but clearly did not occur efficiently at the sensitized $Ru(bpy)_2(dcb)/TiO_2$ interface under these experimental conditions. Later studies revealed that Li^+ cations present in the external acetonitrile electrolyte promoted excited-state injection with yields close to unity for $[Li^+] > 0.1$ M.[36] Other alkali and alkaline earth cations displayed similar behavior in a manner consistent with the size-to-charge ratio of the cation. In the absence of these so-called potential-determining ions the MLCT excited state of $Ru(bpy)_2(dcb)^*/TiO_2$ was remarkably similar to that of the carboxylate form of the sensitizer in fluid solution. However, the relaxation mechanism was dramatically different on TiO_2, particularly at high surface coverages when a large number of excited states were present.

At low excitation irradiances the $Ru(bpy)_2(dcb)^{2+*}/TiO_2$ excited-state decay followed a first-order kinetic model with lifetimes that were very comparable to that measured in fluid CH_3CN, $\tau = 0.8 \pm 0.2$ μs. At higher irradiances where greater than one excited state was formed on each TiO_2 nanocrystallite, excited-state relaxation was second-order, consistent with a triplet−triplet excited-state annihilation reaction. With intermediate irradiances, excited-state relaxation was well described by a parallel first- and second-order kinetic model.[6] While a distribution of rate constants might have been expected in such a heterogeneous environment, dispersive excited-state relaxation kinetics were not required to accurately model the data. Taken together, the kinetic data indicated that the close proximity of the molecular sensitizers promoted rapid intermolecular energy transfer self-exchange until excited-state relaxation occurs or two excited states encounter one another and annihilate. Interestingly, the second-order pathway was not observed for $Os(bpy)_2(dcb)^*/TiO_2$ under the same experimental conditions,[38] presumably because nonradiative decay from the relatively short-lived ($\tau = 50$ ns) excited-state lifetime competed kinetically with self-exchange, thereby lowering the number of hops and the likelihood that two excited states would encounter one another. This observation provided some qualitative insights into energy-transfer dynamics, and the kinetic data provided the first evidence that lateral self-exchange energy transfer was operative in these mesoporous thin film materials.

As the second-order annihilation reaction occurred in parallel with first-order radiative and nonradiative decay, it was not obvious how one would quantify the fraction of excited states that decayed through each pathway. A visual inspection of the temporal data revealed that the second-order pathway was most prevalent at short observation times (when the number of excited states was large) and unimolecular relaxation was dominant when the number of excited states was small (at long observation times). An analytical model was derived that enabled the fraction of excited states that relaxed through each pathway to be determined from the time-resolved absorption data.[38] As would be intuitively expected, the fraction of excited states that followed the second-order pathway increased with the sensitz(er surface coverage and with the number of excited states formed by pulsed light excitation.

Studies with sensitized films that contained both $Ru(bpy)_2(dcb)^{2+}$ and $Os(bpy)_2(dcb)^{2+}$ provided the first direct spectroscopic evidence that lateral energy transfer occurred in these sensitized thin films (Figure 6).[7,39] Energy transfer from

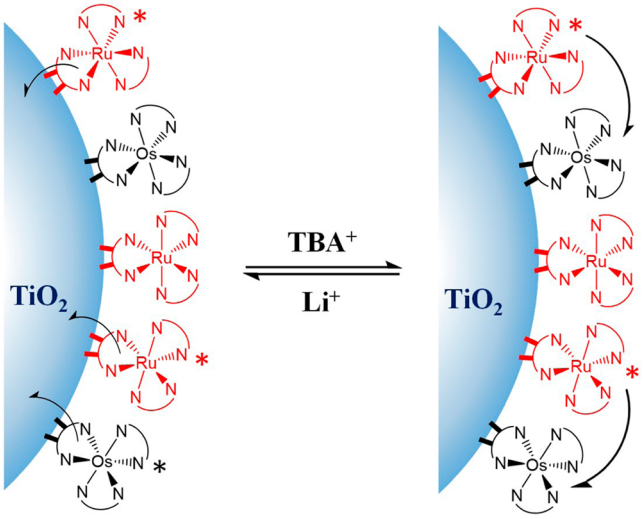

Figure 6. Excited-state electron injection (left) was favored in 0.1 M Li^+, and lateral energy transfer (right) was favored in TBA^+ acetonitrile electrolytes. Adapted with permission from ref 7. Copyright 1999 American Chemical Society.

$Ru(bpy)_2(dcb)^*/TiO_2$ to $Os(bpy)_2(dcb)/TiO_2$ was energetically favored by about 400 meV and occurred with quantum yields near unity when thin films were sensitized with 1:1 Os/Ru sensitizer ratios at saturation surface coverages. The energy-transfer yields were not particularly sensitive to the identity of the solvent that surrounded the thin films (THF, CH_3CN, hexanes, or CCl_4), implying a small contribution from the outer-sphere reorganization energy.[38] When the number of $Os(bpy)_2(dcb)^{2+}$ compounds was much less than that for $Ru(bpy)_2(dcb)^{2+}$, the appearance of energy-transfer product $Os(bpy)_2(dcb)^*/TiO_2$ was rate limited by lateral $Ru(bpy)_2(dcb)^*/TiO_2 + Ru(bpy)_2(dcb)/TiO_2 \rightarrow$ self-exchange. Dexter energy transfer occurs by a double-electron-exchange mechanism, and Marcus theory predicted a self-exchange rate constant of 2×10^{11} s^{-1} at saturation surface coverages. The reorganization energy was abstracted from a Franck−Condon line shape analysis of the corrected photoluminescence spectra, $\lambda = 0.34$ eV, under the assumption of an optimal frequency factor of 10^{13} s^{-1}.

Simulations of lateral self-exchange reactions are inherently complicated by necessary assumptions about packing densities, intermolecular distances, and heterogeneity. Initial simulations were based on an ideal 32×32 planar array of close-packed sensitizers with four (primitive) or six (hexagonal) nearest neighbors with a circular boundary condition that translated excited states that hopped "off" the array to the opposite side where they continued their random walk.[38] The modeling suggested that the hexagonal packing of sensitizers gave better

DOI: 10.1021/acs.langmuir.5b02129
Langmuir 2015, 31, 11164−11178

fits to the experimental data than did the primitive arrangement. The agreement between simulated and experimental data was poor when >10% of the ground states were converted to excited states, behavior attributed to the finite probability that the laser pulse created two excited states adjacent to one another that could annihilate without first undergoing lateral self-exchange.[38]

The Monte Carlo simulations utilized today employ spherical TiO_2 nanocrystallites with sensitizers arranged at van der Waals separation.[5] The initial distribution of excited states (or oxidized sensitizers for hole-hopping self-exchange) is randomly selected, and the probability for hopping to any other sensitizer is calculated using the degeneracy of each hop with an exponential decrease in H_{AB} with β equal to 1 $Å^{-1}$. After each hop the sensitizers are repacked in a hexagonal array, and this process is repeated for a given number of iterations, corresponding to the amount of time until a simulated decay is generated. Minimization of synthetic decays with respect to experiment is then performed with the nearest-neighbor hopping rate constant as the only adjustable parameter. Such modeling has provided an energy-transfer hopping rate of $(120\ ns)^{-1}$ that includes the nearest-neighbor degeneracy and hence $k_{se} = (710\ ns)^{-1}$ for a single self-exchange energy-transfer reaction such as that depicted in eq 2.[5]

III. DIRECT EVIDENCE FOR SELF-EXCHANGE ENERGY AND ELECTRON TRANSFER IN MESOPOROUS TIO_2

Thermal Self-Exchange Electron Transfer. An unexpected cation dependence for $Ru^{III/II}$ self-exchange was observed for $Ru(bpy)_2(dcb)/TiO_2$ (or ZrO_2) under conditions where the oxide thin film had been pretreated with aqueous acid or base solutions prior to surface functionalization and characterization in CH_3CN electrolytes.[14] Cyclic voltammograms showed negligible $Ru^{III/II}$ redox chemistry for base-pretreated $Ru(bpy)_2(dcb)/TiO_2$ in 0.1 M $TBAClO_4$ CH_3CN electrolyte. Interestingly, these same materials displayed significant self-exchange when $LiClO_4$ was used in place of $TBAClO_4$ as the electrolyte. The presence of Li^+ cations led to some surface desorption, suggesting that translational mobility across the TiO_2 surface accounted for the enhanced self-exchange. More recent anisotropy studies described below provide an alternative explanation: Lewis acid cations lower the work terms for electron-transfer self-exchange.[5] In bimolecular redox chemistry in fluid solution the work terms are predominately Coulombic when charged molecules are brought together to form a precursor complex before self-exchange. The restricted translational mobility of sensitizers on mesoporous oxide thin films certainly alters the structure of the precursor complex, and the work terms may involve the motion of surface atoms and/or ions as well as the sensitizer.

Tripodal ruthenium polypyridyl compounds developed by the Galoppini group provided an outstanding opportunity to investigate whether the proximity of the metal center with respect to the interface influenced lateral $Ru^{III/II}$ self-exchange.[26] In one particular study, a tripodal ligand fixed the ruthenium centers about 17 Å from the surface-anchoring carboxylic acid groups (Figure 7). A comparative self-exchange study with $Ru(bpy)_2(dcb)/TiO_2$ revealed D_{app} values that were, within experimental error, the same as that measured for the tripodal sensitizer. Hence there was no evidence that the tripodal structure influenced $Ru^{III/II}$ self-exchange. As the footprint of the tripod on the TiO_2 surface was expected to be about the same size as the Ru trisbiypridyl chelate, the Ru–

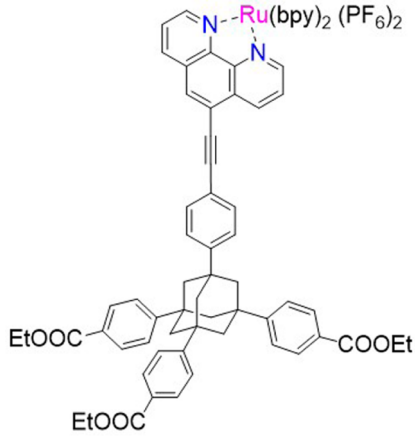

Figure 7. Molecular structure of a tripodal ruthenium compound.

Ru intermolecular distance was expected to be approximately the same for both sensitizers, and this probably underlies the observed behavior. The data indicate that the proximity of the redox-active $Ru^{III/II}$ to the oxide surface was not an important experimental consideration and suggested that the TiO_2 surface did not contribute significantly to the total reorganization energy for self-exchange. Recent theoretical calculations suggest otherwise.[40]

Self-exchange studies of $Ru(bpy)_2(dcbq)/TiO_2$, where dcbq is 4,4′-$(CO_2H)_2$-2,2′-biquinoline, were of particular interest as two separate redox equilibria could be quantified.[13,41] One was a $Ru^{III/II}$ exchange localized on the d orbitals (t_{2g}^5/t_{2g}^6). The second was $[Ru(bpy)_2(dcbq^{0/-})]^{2+/+}$ reduction that involved the π and π^* orbitals of the coordinated dcbq ligand. Note that the corresponding reduction with dcb-containing sensitizers was not easily observed experimentally due to the presence of the large currents and absorption changes associated with the direct reduction of TiO_2. The dcbq ligand is considerably more easily reduced and occurred before significant TiO_2 reduction provided that no potential-determining cations were present in the CH_3CN electrolyte. Chronoabsorptometry studies revealed that $D_{app}(Ru(dcbq^{0/-})) = (3.3 \pm 0.3) \times 10^{-8}$ cm^2/s was more than 10-fold larger than $D_{app}(Ru^{III/II}(dcbq)) = (2 \pm 1) \times 10^{-9}$ cm^2/s. The very different self-exchange rate constants for the two processes were attributed to the fact that the dcbq π^* orbitals were energetically proximate to the redox active states in TiO_2 while the $Ru^{III/II}$ reduction potentials were over 1 eV more positive. It was therefore concluded that the conduction band of TiO_2 mediated the $Ru(dcbq^{0/-})$ self-exchange reaction. In retrospect, the term "conduction band" was unfortunate as it was unclear whether the redox active states in TiO_2 were conduction band electrons or electrons trapped in surface states (perhaps as localized Ti(III) states) residing energetically within the forbidden energy gap; however, a more recent study indicated that conduction band electrons were indeed involved.[46] In any event, the data provided evidence that the redox active states in TiO_2 were important to the $Ru(dcbq^{0/-})$ self-exchange. The reduction of the coordinated dcbq ligand occurred at more positive potentials than does TiO_2 reduction such that electrons injected into TiO_2 from vibrationally hot excited states were trapped on ground-state sensitizers, producing long-lived states that recombined through self-exchange reactions that are described further below.

Interestingly, the reduction of $[Ru(bpy)_2(dcbq)]^{2+}/TiO_2$ was kinetically much slower than was the subsequent oxidation of

DOI: 10.1021/acs.langmuir.5b02129
Langmuir 2015, 31, 11164–11178

Table 1. Summary of TiO_2 Surface-Immobilized Dye Self-Exchange Data Available in the Literature

sensitizer[a]	electrolyte[b]	redox center	D_{app} (cm^2/s)	technique[c]	reference
$[Os(dcb)(bpy)_2]^{2+}$	0.1 M $TBAPF_6/CH_3CN$	$Os^{III/II}$	1.4×10^{-9}	CA	42
$[Ru(dcb)(bpy)_2]^{2+}$	0.1 M $TBAPF_6/CH_3CN$	$Ru^{III/II}$	8×10^{-9}	CA	43
$[MeOTPA\text{-}PO_3Na_2]^{2+}$	$EtMeIm^+Tf2N^-/CH_3CN$ (1:1)	$MeOTPA^{+/0}$	1.1×10^{-7}	CA	11
[PMI-T2-TPA-COOH]	EMITFSI	$TPA^{+/0}$	2.2×10^{-8}	CA	12
$Ru(dcb)(dnb)(NCS)_2$	0.1 M EMITFSI/CH_3CN	$Ru(NCS)^{III/II}$	4.1×10^{-9}	CC	44
	EMITFSI		1.5×10^{-9}	CV	
$Ru(dcb)(dmb)(NCS)_2$	0.1 M $TBAPF_6/CH_3CN$	$Ru(NCS)^{III/II}$	11.4×10^{-9}	IS	
	EMITFSI		3.8×10^{-9}	CV	
$Ru(dcb)(dmb)(CN)_2$	0.1 M $TBAPF_6/CH_3CN$	$Ru^{III/II}$	1.9×10^{-9}	IS	
	EMITFSI		0.09×10^{-9}	CV	
$[Ru(dcb)(dmb)_2]^{2+}$	0.1 M $TBAPF_6/CH_3CN$	$Ru^{III/II}$	0.3×10^{-9}	CV	
$[Ru(dcb)_2(dtdbpy)]^{2+}$	0.1 M EMITFSI/CH_3CN	$Ru^{III/II}$	0.02×10^{-9}	CV	
$[Ru(bpy)_2(dcbq)]^{2+}$	0.1 M $TBAClO_4/CH_3CN$	$Ru^{III/II}$	3.3×10^{-8}	CA	41
		$Ru(dcbq^{0/-})$	2×10^{-9}		
N621 ($Ru(dcb)(dtdbpy)(NCS)_2$)	0.1 M $TBAClO_4/CH_3CN$	$Ru^{III/II}$	1.2×10^{-9}	CA	45
HW456 ($Ru(dcb)(BVTPAbpy)(NCS)_2$)		$TPA^{+/0}$	2.6×10^{-8}		
C1 ($Ru(OMeTPA\text{-}OMepbpy)(H_2tctpy)$)	0.5 M $LiClO_4/CH_3CN$	$Ru^{III/II}$	6.3×10^{-9}	CA	46
C5 ($Ru(OMeTPA\text{-}CF_3pbpy)(H_2tctpy)$)		$MeOTPA^{+/0}$	1.3×10^{-8}		
$Ru(dcb)(dnb)(NCS)_2$	0.1 M $TBAPF_6/CH_3CN$	$Ru^{III/II}$	2.0×10^{-8}	CV	15
$Ru(dcb)(dmb)(NCS)_2$		$Ru^{III/II}$	3.5×10^{-8}		
D131(organic indoline)		$indoline^{+/0}$	2.8×10^{-8}		
D149(organic indoline)		$indoline^{+/0}$	27×10^{-8}		
TT-1(ZnPc)		$Pc^{+/0}$	0.39×10^{-8}		
TT-35(RuPc)		$Pc^{+/0}$	3.9×10^{-8}		
A2(RuPc)		$Pc^{+/0}$	1.7×10^{-8}		
A5(RuPc)		$Pc^{+/0}$	1.3×10^{-8}		

[a]Sensitizer studied where dcb is 4,4′-$(CO_2H)_2$-2,2′-bipyridine, dmb is 4,4′-$(CH_3)_2$-2,2′-bipyridine, dnb is 4,4′-(nonyl)$_2$-2,2′-bipyridine, dtdbpy is 4,4′-ditridecyl-2,2′-bipyridine, TPA is triphenyl amine, PMI is perylenemonoimide, T2 is bithiophene, dcbq is 4,4′-dicarboxylic acid-2,2′-biquinoline, BVTPAbpy is 2,2′-bipyridyl-4,4′-bis(vinyltriphenylamine), pbpy is 6-phenyl-2,2′-bipyridine, H_2tctpy is 4,4′,4′-tricarboxy-2,2′:6′,2″-terpyridine, and Pc is phthalocyanines. [b]Electrolyte used where TBA is tetra-*n*-butyl ammonium, $EtMeIm^+Tf2N^-$ is 1-ethyl-2-methylimidazolium bis(trifluoromethylsulfonyl)imide, and EMITFSI is 1-ethyl-3-methylimidazolium bis(trifluoromethanesulfonyl)amide. [c]Techniques employed include chronoabsorptometry (CA), chronocoulometry (CC), cyclic voltammetry (CV), and impedance spectroscopy (IS).

$[Ru(bpy)_2(dcbq^-)]^+/TiO_2$. Similar rectification was observed for an unsensitized thin film where the blue-black color that accompanied TiO_2 reduction appeared slowly yet disappeared quickly when the potential was stepped to more positive values.[13] This observation suggested that the reduction of the dcbq ligand was rate-limited by electron transport in TiO_2 and occurred only after some fraction of the TiO_2 had already been reduced.

Later studies utilized a naturally occurring hemin that displayed an $Fe^{III/II}$ reduction potential about 300 mV more positive than that of $[Ru(bpy)_2(dcbq^{0/-})]^{2+/+}$.[13] The large extinction coefficient of hemin enabled spectroscopic measurements at ∼1/100 the saturation surface coverages, yet no percolation threshold was observed, indicating that the redox chemistry was indeed mediated by the TiO_2. It was found that the reduction of Fe^{III} to Fe^{II} was much faster than the subsequent oxidation of Fe^{II} back to Fe^{III}. Hence the rectification was in the opposite direction to that observed for $[Ru(bpy)_2(dcbq^{0/-})]^{2+/+}$. Since it was thermodynamically downhill for the electrons in TiO_2 to reduce Fe^{III} to Fe^{II}, unlike the reduction of $[Ru(bpy)_2(dcbq)]^{2+}$, the kinetics were not limited by the need to build up a concentration of trapped electrons. When the potential was stepped back to oxidize heme back to hemin ($Fe^{II} \rightarrow Fe^{III}$), the electrons in TiO_2 were quickly abstracted, and since the $Fe^{III/II}$ reduction potential was sufficiently below that of the unfilled TiO_2 acceptor states, they remained trapped in their oxidized forms. In principle, if all of the TiO_2 surface states energetically proximate to the $Fe^{III/II}$ reduction potential were absent and the surface coverage was below the percolation threshold, then the oxidized hemes would remain trapped on TiO_2 indefinitely. In practice, the redox chemistry took minutes to complete.

The rectification behavior appears to be limited to cases where the semiconductor mediates charge transfer through the direct involvement of TiO_2 trap and/or conduction band states and is absent for those that have formal reduction potentials of >0.5 V vs NHE.[47] Spectroelectrochemical studies have revealed no evidence of surface states within the anatase TiO_2 thin films at these positive potentials. Presumably if one were able to control the self-exchange reactivity at very positive applied potentials the valence band states could be accessed. With amorphous TiO_2 thin films deposited by atomic layer deposition, a recent study indicates that surface states can mediate hole transfer reactions at the potentials relevant to water oxidation, > 1.23 V vs NHE.[48] High levels of n-type doping can produce degenerate oxide materials, where the Fermi level is within the metal oxide conduction band, resulting in metal-like behavior utilized as transparent conductive oxides, TCOs, for a variety of applications.[49,50] In single-crystal rutile photoelectrochemistry under forward bias conditions, it is well documented that the partially reduced TiO_2 begins to behave very much like a metallic electrode, and at a negative applied potential, the mesoporous anatase TiO_2 thin film appears to behave similarly. Reversible redox chemistry has been reported

DOI: 10.1021/acs.langmuir.5b02129
Langmuir 2015, 31, 11164−11178

in cyclic voltammograms for example.[51] Collectively, this data shows that different TiO_2 preparations, doping levels, and/or applied potentials can produce redox active states in the material that must be taken into account for self-exchange studies.

Self-exchange reactions that have been reported in the literature are given in Table 1. The range of D_{app} values for hole hopping is from 3×10^{-9} to 1×10^{-7} cm^2/s. The tabulated data are for cases where self-exchange is the only mechanism involved; i.e., there was no evidence of mediation by the oxide material itself. While comparison between different references should be done with caution, it appears that $TPA^{+/0}$ self-exchange is 1 to 2 orders of magnitude faster than $Ru^{III/II}$ self-exchange.

An issue that concerns lateral hole hopping is the assertion in the Introduction and throughout the text that self-exchange electron transfer occurs with $\Delta G^\circ = 0$ in these mesoporous TiO_2 thin films. Heterogeneity may induce a distribution of sensitizer environments with a corresponding distribution of reduction potentials that could provide a free-energy gradient for self-exchange. The factors that control redox equilibrium at molecular oxide interfaces remain relatively poorly understood. Indeed molecular redox chemistry at these interfaces often does not obey the Nernst equation. The same spectroelectrochemical measurements that provide kinetic information on lateral hole hopping have also been performed under steady-state conditions to quantify this redox equilibria. In such experiments, the quasi-Fermi level of the mesoporous film is controlled with an applied bias, and absorption spectra are measured in the visible and near-infrared regions. The spectral data is reformulated as a chemical capacitance. An example is shown in Figure 8 for the indicated sensitizer that has a $Ru^{III/II}$ and a triphenyl amine, $TPA^{+/0}$, redox reactivity.[52] The peak of the distributions corresponds to the equilibrium potential at which equal concentrations of the two redox states are present and is taken as a measure of the formal reduction potential.

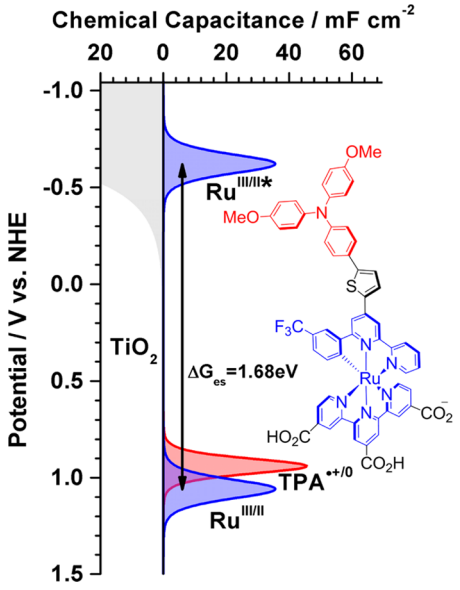

Figure 8. Interfacial energetics for the indicated sensitized mesoporous TiO_2 thin film. Note that this sensitizer displays $Ru^{III/II}$ and $TPA^{+/0}$ redox activity. Adapted with permission from ref 52. Copyright 2012 American Chemical Society.

While the capacitance distributions corresponding to the $Ru^{III/II}$ and $TPA^{+/0}$ redox equilibria appear to be Gaussian, they are not.[53] A useful analytical expression introduces a nonideality factor into the Nernst equation that is given in eq 6, where θ is the cumulative fraction of molecules in a given redox state, E° is the formal reduction potential, and a is the nonideality factor. When a is unity, Nernstian behavior results, and a 59 mV change in applied potential, E_{app}, will give rise to an order-of-magnitude change in concentration for a single electron transfer at room temperature.

$$\theta(E_{app}) = \frac{1}{1 + 10^{E_{app} - E^\circ / a \times 59\ mV}} \quad (6)$$

For the data shown in Figure 8, $a = 1.3 \pm 0.1$ for the $Ru^{III/II}$ process and $a = 1.1 \pm 0.1$ for the triphenyl amine redox chemistry.[52] The TPA group is expected to be further from the surface, and its more ideal redox behavior gives credence to the idea that the nonideality originates from the TiO_2. In a recent study with a cobalt porphyrin, the $Co^{III/II}$ redox chemistry behaved more ideally than did $Co^{II/I}$.[53] Such behavior was not easily rationalized with a model wherein intermolecular interactions influence the reduction potentials of catalysts that have not yet been reduced, i.e., Frumkin behavior. This was further corroborated by the fact that both the ideality factors and the formal reduction potentials were practically surface-coverage-independent. Furthermore, while an underlying Gaussian distribution of energy states may induce a normal distribution of redox potentials and hence nonunity ideality factors, this would require very different distributions for the same compound. Cobalt porphyrins prefer coordination numbers of 4, 5, and 6 when in the formal oxidation states of I, II, and III, respectively; however, this coordination chemistry was not believed to be the main contributor to the nonideality. Analysis in $LiClO_4$ provided fractional potential drops of only ~15% for $Co^{III/II}$, which was noticeably larger for the $Co^{II/I}$ equilibrium, ~ 45%. The $Co^{II/I}$ redox chemistry occurred at potentials where TiO_2 reduction also occurred, and this was thought to be the origin of the large potential drop. The ideality factors and hence applied potential drops were found to be invariant with the surface coverage.

In summary, the close inspection of redox equilibrium at sensitized TiO_2 interfaces often reveals non-Nernstian behavior that raises significant questions about the true formal reduction potentials and the origin(s) of the nonideal behavior. Models based on distributions of formal reduction potentials,[54] intermolecular interactions (i.e., Frumkin-like behavior),[55] and electric field effects[56] have been broadly invoked to model the observed data with a variety of electrode materials. At TiO_2 interfaces, the electric field contributions appear to be most significant; however, the number of experimental studies remains quite limited and deserves further study.[46,53]

Light-Driven Self-Exchange. There have been several occasions where lateral self-exchange reactions were initiated with light. An early example occurred when $Ru(bpy)_2(dcbq)/TiO_2$ (and related biquinoline-containing sensitizers) was excited with pulsed light.[41,57] A very long-lived transient species was discovered that returned to ground-state products on a tens of seconds time scale. Indeed, the return to ground-state products was so slow that it could be monitored in a standard UV−vis spectrometer. Spectral analysis revealed that the long-lived transients were due to the presence of $Ru^{III}(bpy)_2(dcbq)/TiO_2$ and $Ru(bpy)_2(dcbq^-)/TiO_2$ in equal concentrations. A model was proposed wherein excited-state

DOI: 10.1021/acs.langmuir.5b02129
Langmuir 2015, 31, 11164−11178

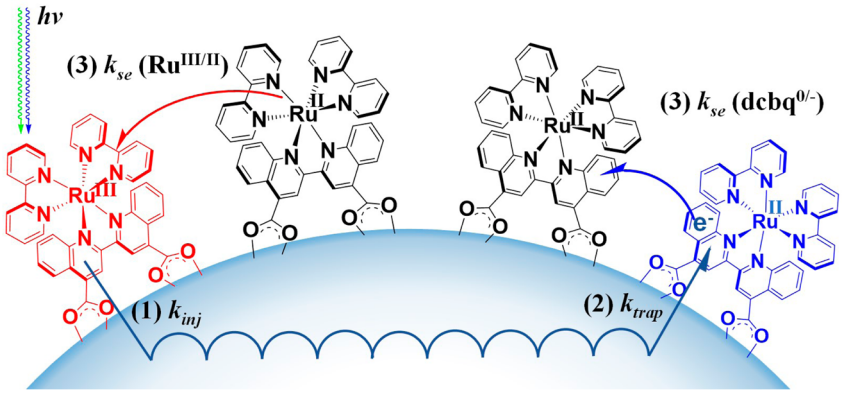

Figure 9. Lateral $Ru^{III/II}$ and $dcbq^{0/-}$ self-exchange reactions of $Ru^{II}(bpy)_2(dcbq)/TiO_2$ after light excitation: (1) electron injection, (2) electron trapping, and (3) self-exchange hole hopping to form a close encounter of $Ru^{III}(bpy)_2(dcbq)$ and $Ru^{II}(bpy)_2(dcbq^-)$. Adapted with permission from ref 41. Copyright 2006 American Chemical Society.

injection occurred with a rate constant of $k_{inj} > 10^8$ s^{-1} from vibrationally hot (upper) excited states followed by rapid trapping of the injected electron by a ground-state sensitizer with a rate constant of k_{trap} (Figure 9). Recall that in the absence of potential-determining cations the dcbq ligand is reduced before TiO_2 such that it is thermodynamically favorable for an injected electron to reduce a ground-state sensitizer. The recombination mechanism was asserted to be rate-limited by lateral self-exchange until a close encounter with the oxidized and reduced forms enabled electron transfer to yield ground-state products. The kinetics were well modeled by a stretched exponential function that yielded a rate constant of $k_{se} = (8 \pm 5) \times 10^5$ s^{-1} and $\beta = 0.25 \pm 0.05$, corresponding to a Levy distribution of rate constants that was so broad that they were of questionable value. The $Ru^{III}(dcbq)$ $(bpy)_2/TiO_2$ + $Ru(dcbq^-)$ $(bpy)_2/TiO_2$ reaction occurred with a driving force larger than that stored in the thermally equilibrated excited state. Hence, the rapid trapping of electrons injected from upper excited states is relevant toward exceeding the well-known Schockly−Queisser limit. Intermolecular electron transfer formally occurs from an electron localized on a dcbq ligand to the Ru^{III} d orbitals. This could yield two ground-state sensitizers. However, for $Ru(bpy)_3^{2+*}$ the corresponding reaction occurs so deeply in the Marcus kinetic inverted region that instead an MLCT excited state and a ground state are formed, providing the basis for many electroluminescence assays.[58−60] Efforts to observe the delayed photoluminescence that would result from self-exchange charge transfer followed by electron transfer to yield an MLCT excited state are continuing yet remain elusive at these TiO_2 interfaces.

While the above example produced charge-separated states that stored more free energy than did the excited state and was hence of relevance to the Shockley−Queisser limit, the quantum yields for their formation were very low, $\phi < 0.05$. Under the conditions where this behavior was observed, the thermally equilibrated excited state did not inject electrons, and the low yields were due to inefficient injection from upper excited states. Bignozzi and his group circumvented this issue by identifying conditions under which the equilibrated excited state of sensitizer $[Ru(dcb)_2(CN)_2]$ was quantitatively injected into TiO_2.[61] A mixed-valence electron acceptor $[(ina)\text{-}Ru^{III}(NH_3)_4(NC)Ru^{II}(CN)_5]^-$, where ina is pyridine-4-carboxylic (isonicotinic) acid, was coanchored to the surface at about 25% of the saturation surface coverage. After steady-state illumination, recombination of the oxidized sensitizer and the reduced acceptor required around 80 min. Maintaining the mixed-valence acceptor's surface coverage below the percolation threshold helped to ensure that the predominant self-exchange pathway was by $[Ru^{III/II}(dcb)_2(CN)_2]^{+/0}$ hole hopping. There was some evidence that superoxide acted as a mobile electron shuttle that facilitated charge recombination. When the sensitized thin film was coated with poly(methyl methacrylate) (PMMA), recombination was inhibited and required more than 36 h. The intense color changes that accompanied this redox chemistry may have application as photochromic materials.

The previously described Ru carbene sensitizers with a pendent triphenyl amine (TPA) group have provided new opportunities for the study of light-driven self-exchange reactions.[46] The $Ru^{III/II}$ and $TPA^{+/0}$ reduction potentials can be independently tuned such that either the metal center or the TPA group was oxidized more easily. Light excitation of a sensitized thin film where the ruthenium center of every sensitizer within the thin film was completely oxidized, TPA-Ru^{III}/TiO_2, resulted in rapid "remote" excited-state injection, $k_{inj} > 10^8$ s^{-1} to yield TPA^+-$Ru^{III}/TiO_2(e^-)$. The large number of Ru^{III} acceptors on the surface resulted in rapid back electron transfer to yield a fully reduced sensitizer, i.e., TPA-Ru^{II}/TiO_2, that was present in equal numbers with the fully oxidized sensitizers. This state stored about 120 meV of free energy and recombined by lateral self-exchange on a 10^{-3}−10^{-6} s time scale. Computational modeling of self-exchange reactions was accomplished with a 3 × 3 × 3 array of anatase nanocrystallites with saturation sensitizer surface coverage. Monte Carlo simulation was carried out to model the kinetics of the lateral self-exchange reaction of TPA-Ru^{II}/TiO_2 + TPA^+-Ru^{III}/TiO_2 → 2TPA-Ru^{III}/TiO_2. The excitation intensity was varied so that the average number of electron (TPA-Ru^{II}/TiO_2) and hole (TPA^+-Ru^{III}/TiO_2) pairs per TiO_2 nanoparticle created by the laser pulse was one to five (Figure 10). An average hopping rate of $(130\ ns)^{-1}$ was abstracted, indicating that on average an electron or hole could circumnavigate a single TiO_2 nanocrystal once before charge recombination.

In a light-driven electron self-exchange reaction on a p-type semiconductor, NiO was also observed by Gardner and co-workers in an attempt to accumulate two reducing equivalents on a catalyst.[62] An excited coumarin-343 dye was injected into a hole in NiO upon visible-light excitation. The reduced coumarin transferred electrons to neighboring dye molecules until it encountered a coadsorbed catalyst where reduction was

DOI: 10.1021/acs.langmuir.5b02129
Langmuir 2015, 31, 11164−11178

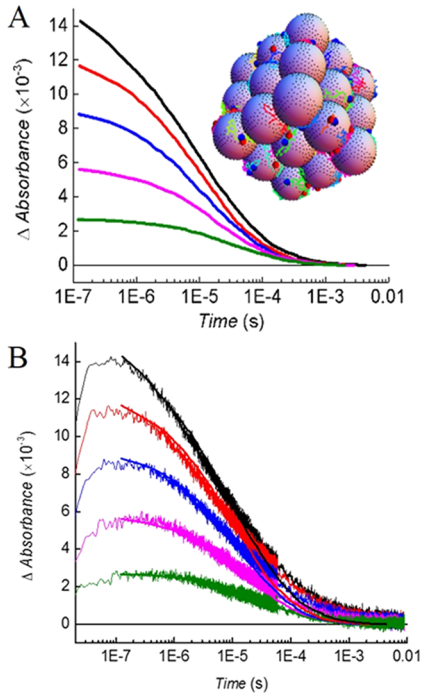

Figure 10. Monte Carlo simulations of a 3 × 3 × 3 nanocrystal array of absorption transients corresponding to hole hopping at five different initial concentrations (A) and experimental data with overlaid array simulations (B). Adapted with permission from ref 46. Copyright 2014 American Chemical Society.

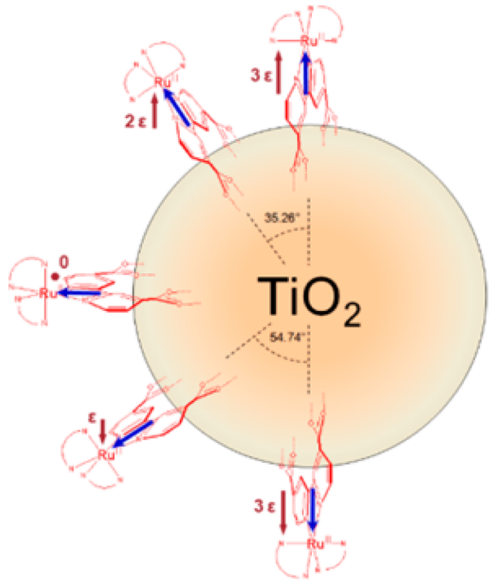

Figure 11. Depiction of the anisotropy experiment with a sensitized TiO_2 nanocrystallite under vertically polarized light excitation. The blue arrows indicate the sensitizer's lowest-energy charge-transfer dipole moment, and the magnitude of the overlap between the dipole moment and the excitation polarization vector is given with dark-brown arrows, where ε is the absorption coefficient measured in fluid solution. Adapted with permission from ref 5. Copyright 2011 American Chemical Society.

favored by ~500 meV. The charge-separated state that was formed had a lifetime of up to 100 μs. Rapid hole hopping away from the injection site was hypothesized to be critically important for efficient catalyst activation.

Transient Anisotropy. Excited-state injection from a sensitizer into TiO_2 is known to occur on ultrafast time scales under many different experimental conditions.[63] The question of whether the oxidized sensitizer remained "glued" to the injection site or could hop away by lateral self-exchange was addressed recently by time-resolved absorption anisotropy. The anisotropy experiment is most easily described with the aid of an idealized TiO_2 nanocrystallite with the surface-anchored Ru polypyridyl sensitizer's lowest-energy charge-transfer transition dipole moment depicted by singly degenerate vectors (blue arrows) (Figure 11).[5] An anisotropic molecular subpopulation is generated by photoselection of the surface-anchored sensitizers with vertically polarized laser excitation. The magnitude of the overlap between the molecular transition dipole moments and the polarization vector of the excitation light (polarized vertically and propagating in the plane of the page) is depicted as thick brown arrows, where ε is the extinction coefficient measured in isotropic fluid solution. This figure illustrates that sensitizers positioned closer to the north and south poles of each nanocrystallite are preferentially photoexcited relative to those near the equator. The photoselected transition dipole moments in the laboratory frame of reference are expected to move little due to molecular or nanocrystallite diffusion; however, the detected transition dipole moments will change for sensitizers that participate in lateral self-exchange reactions.

Significant anisotropy was observed in the time-resolved absorption and photoluminescence of Ru(dcb) $(dtb)_2/TiO_2$, where dtb is 4,4′-(*tert*-butyl)$_2$-2,2′-bipyridine, due to lateral self-exchange reactions across the TiO_2 surface.[5] The assignment to lateral self-exchange was supported by surface coverage and temperature studies, but the following observation was the most compelling. Under conditions where the excited-state injection yield was less than unity, the anisotropy decays associated with energy and hole hopping on the same sensitized thin film occurred at drastically different rates. If the anisotropy changes were due to translation/rotation of the sensitizers, then one would expect that the excited state and the oxidized state would do so at nearly identical rates, contrary to what was observed experimentally. An approximate order-of-magnitude difference in the correlation time (θ) between self-exchange energy- and hole-transfer reactions was measured. For example, after light excitation of Ru(dcb) $(dtb)_2/TiO_2$, θ_{ent} = 3.3 μs and θ_{h+} = 17 μs. The temperature dependence for energy transfer self-exchange was negligibly small over a 77−283 K range, further indicating that translational mobility of the sensitizers did not underlie the observed loss in anisotropy.

With pulsed-laser excitation, anisotropy measurements provide kinetic information on self-exchange dynamics on very short time scales. An advantage of the anisotropy measurements over the electrochemical methods is that an external electrolyte is not needed and lateral hole-hopping dynamics can therefore be quantified for a wider range of experimental conditions. A difference between the two methods is that the spectroscopic approach reports on self-exchange under conditions where competitive $TiO_2(e^-) \rightarrow S^+$ back electron transfer is operative. The presence of injected electrons polarizes the interface, and this may significantly influence the lateral self-exchange reactivity from that measured in the dark. The anisotropy approach is also amenable to all sensitizers capable of excited-state injection, including organic dyes and transition-metal compounds based on $Cu^{II/I}$, $Ru^{III/II}$, and $Fe^{III/II}$ as well as the newly discovered $Co^{II/I}$ compounds.[64]

DOI: 10.1021/acs.langmuir.5b02129
Langmuir 2015, 31, 11164−11178

Interestingly, the anisotropy decay for $Ru(dtb)_2(dcb)/TiO_2$ was absent in neat CH_3CN but was clearly observed when the concentration of $LiClO_4$ in acetonitrile exceeded about 10 mM. In contrast, significant self-exchange was evident for *cis*-Ru(dnb) (dcb) $(NCS)_2$ (Z907), where dnb is 4,4′-dinonyl-2,2′-bipyridyl, whether an electrolyte was present or not. It was postulated that ion compensation was necessary for dicationic $[Ru(dtb)_2(dcb)]^{2+}$ whereas it was not as important for neutral Z907 even though it was appreciated that the carboxylic acid groups were present as carboxylates on the TiO_2 surface.

Time-resolved anisotropy data for two widely studied sensitizers, $Z907/TiO_2$ and *cis*-$Ru(dcb)_2(NCS)_2$ $(N3/TiO_2)$, were quantified and are shown in Figure 12. Density functional

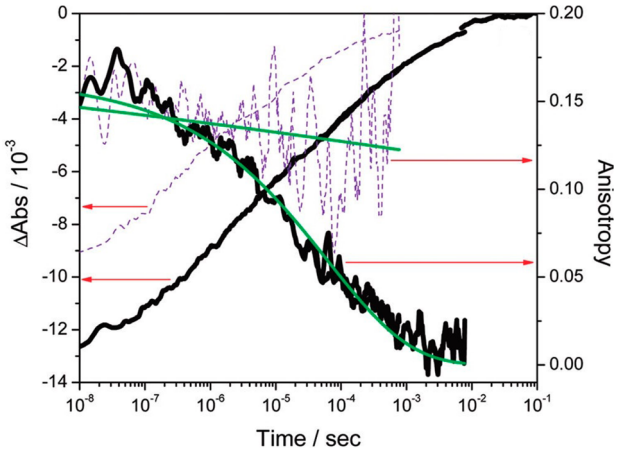

Figure 12. Transient absorption difference magic-angle (left axis) and anisotropy (right axis) changes for *cis*-Ru(dnb) (dcb) $(NCS)_2/TiO_2$ (black, solid) and *cis*-$Ru(dcb)_2(NCS)_2/TiO_2$ thin films immersed in neat acetonitrile monitored at 465 nm after pulsed laser excitation. Overlaid in green on the anisotropy kinetics are fits to a stretched exponential function. Reprinted in part with permission from ref 5. Copyright 2011 American Chemical Society.

theory provided evidence that the highest occupied molecular orbital (HOMO) had both Ru and NCS^- character such that significant electron density was lost from the sulfur atom when these sensitizers were oxidized.[65] Within the charge recombination time window, $Z907/TiO_2$ showed complete anisotropy decay with highly skewed kinetics that were well described by the stretched exponential function from which an average hole-hopping correlation time of 9.6 μs was abstracted. However, little to no anisotropy decay was observed for $N3/TiO_2$ over the same time. A faster hole-hopping rate for $Z907/TiO_2$ relative to that for $N3/TiO_2$ was consistent with reports by Wang and co-workers, who implicated the surface orientation of the *cis*-$Ru(NCS)_2$ core as a key parameter.[44] Computational studies combined with FTIR data indicated that N3 was anchored to TiO_2 through one carboxylate group from each dcb ligand; such surface binding resulted in poor intermolecular alignment for self-exchange.[44,66] In contrast, both carboxylate groups on the dcb ligand of $Z907/TiO_2$ were anchored to the surface, and this provided a stacking configuration that promoted rapid intermolecular hole transfer. Interestingly, the coordination of Hg^{2+} to the ambidentate NCS^- ligands was also shown to slow hole hopping. As the time-resolved anisotropy measurements were made on nanosecond and longer time scales and the chronoabsorptometry data were acquired on much slower milliseconds time scales that required interna-

nocrystallite hopping, it was not at all obvious that these two techniques would provide self-consistent data. Nevertheless, the agreement here suggests that the spectroscopic and electrochemical techniques can provide complementary information on hole hopping on very different time scales.[5]

IV. CONCLUSIONS AND FUTURE PERSPECTIVES

Lateral charge and energy-transfer reactions between molecules anchored to mesoporous oxide thin films have been known to occur for about 20 years. The most recent studies have revealed that both the reorganization energy and the intermolecular electronic coupling are acutely sensitive to the molecular details of the interface. The use of time-resolved anisotropy techniques enables lateral self-exchange reactions to be probed on short time scales and in a wide variety of environments. Taken together, these advances provide new opportunities for the characterization of fundamental aspects of the self-exchange reactions. Key questions that remain to be addressed for energy and electron self-exchange in mesoporous oxide thin films include the following: (1) What role does outer-sphere reorganization truly play? Can self-exchange occur efficiently in the absence of solvent or electrolyte? Does oxide surface chemistry contribute to the reorganization energy, and if so, can this be understood on a molecular level? (2) To what extent can the sensitizer structure be used to tune intermolecular electronic coupling H_{AB}? Do bulky ligands lower electronic coupling? Can theory and/or the orientation of frontier orbitals be utilized to predict H_{AB}? (3) Does electron spin play a role? Are spin conservation rules relaxed at oxide interfaces? (4) How do highly doped metal oxide materials, localized trap states, and/or the valence and conduction bands mediate self-exchange? (5) Does translational mobility on an oxide surface enhance self-exchange? Will nonrigid spacer groups between the surface anchors and the sensitizers influence self-exchange? Do surface linkages that allow hopping and diffusion follow predicted mechanisms?[35] (6) Can protons, ions, atoms, or molecules be translated across metal oxide surfaces by similar self-exchange pathways?

Whether intermolecular self-exchange reactions occurring on oxide surfaces can be exploited for practical applications remains unknown. The dramatic color changes that often accompany the redox chemistry may have application in electrochromic and/or photochromic devices. However, the application that has garnered the most attention and motivated most of the described studies is in solar energy conversion that includes both electrical power generation in DSSCs and related hybrid organic−inorganic photovoltaics as well as solar fuel prouction in what have been termed dye-sensitized photoelectrosynthesis cells (DSPEC).[67]

Dye-Sensitized Solar Cells (DSSCs). The high-surface-area mesoporous nanocystalline TiO_2 (anatase) thin films first reported by Grätzel and O'Regan represented the first time in which an interpenetrating network of electron acceptors (mesoporous TiO_2) and donors (iodide-containing electrolyte) was successfully employed for solar cell applications.[16] Today many classes of interpenetrating networks have been tested in so-called hybrid solar cells,[68] yet these mesoporous TiO_2 thin films remain unrivaled in their ability to quantitatively accept excited-state electrons and transport them over large micrometer distances without significant recombination.

The weak link continues to be the hole-transport material. In DSSCs, these represent the redox mediators in an electrolyte that regenerate the dye after excited-state injection and

DOI: 10.1021/acs.langmuir.5b02129
Langmuir 2015, 31, 11164−11178

subsequently diffuse through the mesopores to a metallic electrode where they are reduced to complete the electrical circuit. The redox mediators identified to date either waste significant free energy (e.g., LiI/I_2 electrolytes), undergo efficient unwanted recombination with TiO_2 electrons (e.g., inorganic solids such as CuSCN and NiO, organic donors (Spiro-OMeTAD), and polymeric hole conductors (polythiophene, PEDOT, etc.)), or suffer from poor solubility with resultant mass-transport limitations at high irradiances (e.g., $[Co^{III/II}(bpy)_3]^{3+/2+}$ solutions).[69] A potentially transformative idea would be to translate the oxidized sensitizers (i.e., holes) to the counter electrode by lateral intermolecular self-exchange electron transfer within the molecular layer by hole hopping. In other words, remove the redox mediator altogether and collect the oxidizing equivalents from sensitizers that undergo hole hopping to the metallic electrode. The lack of systematic studies under conditions where unwanted charge recombination reactions with injected electrons are operative makes it difficult to determine whether efficient solar cells could be fabricated in this way. Success may ultimately require covalent links or controlled aggregation between the sensitizers to increase electronic coupling and turn on adiabatic hole-hopping pathways. If successful, such DSSCs would be expected to produce larger open-circuit photovoltages that would not necessarily require a liquid junction and hence represent an area ripe for future studies.

Dye-Sensitized Photoelectrosynthesis Cells (DSPEC). After excited-state injection occurs, the oxidized sensitizer that is formed can transfer an oxidizing equivalent to a catalyst capable of driving multi-electron-transfer reactions to provide solar fuels that can be stored and utilized at another time. Such cells have been termed dye-sensitized photoelectrosynthesis cells or DSPECs, and the quintessential example would efficiently split water into molecular oxygen and hydrogen gases. Water oxidation requires that four oxidizing equivalents be transferred to a single catalyst capable of driving the reaction. The holes have been delivered to the catalyst by lateral hole hopping from oxidized sensitizers, and preliminary data indicates that this can be accomplished. Indeed, there is some evidence that multiple redox equivalents can be collected on a single catalytic site.[70,71] This too represents a research area ripe for future research.

Lateral energy transfer may be exploited in either DSSCs or DSPECs in a fashion similar to nature's antenna effect.[72,73] Intermolecular energy transfer would enable thinner mesoporous films to be utilized. In addition, materials with inherently low surface areas, such as nanotube and nanowire arrays, could be efficiently sensitized to visible light. As the reorganization energies associated with energy-transfer self-exchange are expected to be much smaller than that for electron transfer, it may ultimately be more efficient for an excited state to find and activate a catalyst than for an oxidized molecule. When energy-transfer self-exchange is rapid relative to excited-state relaxation, a very small number of catalytic sites may be capable of completely quenching the excited state in a manner somewhat akin to the superquenching mechanisms that have been exploited for chemical sensing.[74] Taken together, there exist many exciting opportunities to exploit lateral self-exchange reactions for energy applications.

AUTHOR INFORMATION

Notes

The authors declare no competing financial interest.

Biographies

Ke Hu was born and grew up in Shanghai, China. He did his undergraduate study in chemistry at Fudan University in Shanghai, where he performed thin film Li ion battery research under the supervision of Professor Zhengwen Fu and finished his B.S. thesis with Professor Tao Yi on the research of diarylethene photoswitches in 2010. He earned a Ph.D. in chemistry under the mentorship of Professor Gerald J. Meyer at Johns Hopkins University in 2014 with thesis work focused on the fundamental understanding of electron-transfer processes in DSSCs. Ke is currently a postdoctoral associate with Professor Thomas J. Meyer and is working on photodriven water oxidation in dye-sensitized photoelectrosynthesis cells in the UNC Energy Frontier Research Center.

Gerald J. Meyer (Jerry) received his B.S. degrees in chemistry and mathematics at the State University of New York at Albany (SUNY—Albany). His undergraduate research focused on synthesis and low-temperature copper dioxygen chemistry under the supervision of Michael Haka and Yilma Gutneh in the laboratories of Kenneth D. Karlin. Jerry went on to the University of Wisconsin at Madison, where he earned a Ph.D. in chemistry under the tutelage of Arthur B. Ellis with a particularly valuable collaboration with George Lisensky. His dissertation focused on interfacial acid–base chemistry that altered the depletion layers in illuminated II–VI and III–V semiconductor materials. After a brief postdoctoral appointment with Thomas J. Meyer, he began his independent career in the Chemistry Department at Johns Hopkins University, where he remained for 22 years (1991–2013). Jerry is now a professor of chemistry at the University of North Carolina—Chapel Hill, where he serves as Deputy Director of the UNC Energy Frontier Research Center: Center for Solar Fuels.

ACKNOWLEDGMENTS

This research is primarily supported by the National Science Foundation (NSF) under award CHE-1465060 (to G.J.M.),

DOI: 10.1021/acs.langmuir.5b02129
Langmuir 2015, 31, 11164–11178

and the hole-hopping studies for water oxidation (K.H.) were supported as part of the UNC EFRC: Center for Solar Fuels, an Energy Frontier Research Center funded by the U.S. Department of Energy (DOE), Office of Science, Basic Energy Sciences BES, under award DE-SC0001011.

REFERENCES

(1) Sutin, N. Nuclear, electronic, and frequency factors in electron transfer reactions. *Acc. Chem. Res.* **1982**, *15* (9), 275−282.
(2) Weaver, M. J. Dynamical solvent effects on activated electron-transfer reactions: principles, pitfalls, and progress. *Chem. Rev.* **1992**, *92* (3), 463−480.
(3) Swaddle, T. W. Homogeneous versus Heterogeneous Self-Exchange Electron Transfer Reactions of Metal Complexes: Insights from Pressure Effects. *Chem. Rev.* **2005**, *105* (6), 2573−2608.
(4) Ardo, S.; Meyer, G. J. Direct Observation of Photodriven Intermolecular Hole Transfer across TiO2 Nanocrystallites: Lateral Self-Exchange Reactions and Catalyst Oxidation. *J. Am. Chem. Soc.* **2010**, *132* (27), 9283−9285.
(5) Ardo, S.; Meyer, G. J. Characterization of Photoinduced Self-Exchange Reactions at Molecule-Semiconductor Interfaces by Transient Polarization Spectroscopy: Lateral Intermolecular Energy and Hole Transfer across Sensitized TiO2 Thin Films. *J. Am. Chem. Soc.* **2011**, *133* (39), 15384−15396.
(6) Kelly, C. A.; Farzad, F.; Thompson, D. W.; Meyer, G. J. Excited-State Deactivation of Ruthenium(II) Polypyridyl Chromophores Bound to Nanocrystalline TiO2Mesoporous Thin Films. *Langmuir* **1999**, *15* (3), 731−737.
(7) Farzad, F.; Thompson, D. W.; Kelly, C. A.; Meyer, G. J. Competitive Intermolecular Energy Transfer and Electron Injection at Sensitized Semiconductor Interfaces. *J. Am. Chem. Soc.* **1999**, *121* (23), 5577−5578.
(8) Marcus, R. A.; Sutin, N. Electron transfers in chemistry and biology. *Biochim. Biophys. Acta, Rev. Bioenerg.* **1985**, *811* (3), 265−322.
(9) Vaissier, V.; Barnes, P.; Kirkpatrick, J.; Nelson, J. Influence of polar medium on the reorganization energy of charge transfer between dyes in a dye sensitized film. *Phys. Chem. Chem. Phys.* **2013**, *15* (13), 4804−4814.
(10) Vaissier, V.; Mosconi, E.; Moia, D.; Pastore, M.; Frost, J. M.; De Angelis, F.; Barnes, P. R. F.; Nelson, J. Effect of Molecular Fluctuations on Hole Diffusion within Dye Monolayers. *Chem. Mater.* **2014**, *26* (16), 4731−4740.
(11) Bonhôte, P.; Gogniat, E.; Tingry, S.; Barbé, C.; Vlachopoulos, N.; Lenzmann, F.; Comte, P.; Grätzel, M. Efficient Lateral Electron Transport inside a Monolayer of Aromatic Amines Anchored on Nanocrystalline Metal Oxide Films. *J. Phys. Chem. B* **1998**, *102* (9), 1498−1507.
(12) Wang, Q.; Zakeeruddin, S. M.; Cremer, J.; Bäuerle, P.; Humphry-Baker, R.; Grätzel, M. Cross Surface Ambipolar Charge Percolation in Molecular Triads on Mesoscopic Oxide Films. *J. Am. Chem. Soc.* **2005**, *127* (15), 5706−5713.
(13) Staniszewski, A.; Morris, A. J.; Ito, T.; Meyer, G. J. Conduction band mediated electron transfer across nanocrystalline TiO2 surfaces. *J. Phys. Chem. B* **2007**, *111* (24), 6822−6828.
(14) Qu, P.; Meyer, G. J. Proton-Controlled Electron Injection from Molecular Excited States to the Empty States in Nanocrystalline TiO2. *Langmuir* **2001**, *17* (21), 6720−6728.
(15) Moia, D.; Vaissier, V.; Lopez-Duarte, I.; Torres, T.; Nazeeruddin, M. K.; O'Regan, B. C.; Nelson, J.; Barnes, P. R. F. The reorganization energy of intermolecular hole hopping between dyes anchored to surfaces. *Chem. Sci.* **2014**, *5* (1), 281−290.
(16) O'Reagen, B.; Gratzel, M. A. Low-Cost, High-Efficiency Solar Cell Based on Dye-Sensitized Colloidal Ti0(2) Films. *Nature* **1991**, *353* (6346), 737.
(17) Vlachopoulos, N.; Liska, P.; Augustynski, J.; Graetzel, M. Very efficient visible light energy harvesting and conversion by spectral sensitization of high surface area polycrystalline titanium dioxide films. *J. Am. Chem. Soc.* **1988**, *110* (4), 1216−1220.
(18) Anderson, S.; Constable, E. C.; Dare-Edwards, M. P.; Goodenough, J. B.; Hamnett, A.; Seddon, K. R.; Wright, R. D. Chemical modification of a titanium (IV) oxide electrode to give stable dye sensitisation without a supersensitiser. *Nature* **1979**, *280* (5723), 571−573.
(19) Connor, P. A.; Dobson, K. D.; McQuillan, A. J. Infrared Spectroscopy of the TiO2/Aqueous Solution Interface. *Langmuir* **1999**, *15* (7), 2402−2408.
(20) Young, A. G.; McQuillan, A. J. Adsorption/Desorption Kinetics from ATR-IR Spectroscopy. Aqueous Oxalic Acid on Anatase TiO2. *Langmuir* **2009**, *25* (6), 3538−3548.
(21) Meyer, T. J.; Meyer, G. J.; Pfennig, B. W.; Schoonover, J. R.; Timpson, C. J.; Wall, J. F.; Kobusch, C.; Chen, X.; Peek, B. M. Molecular-Level Electron Transfer and Excited State Assemblies on Surfaces of Metal Oxides and Glass. *Inorg. Chem.* **1994**, *33* (18), 3952−3964.
(22) Argazzi, R.; Bignozzi, C. A.; Heimer, T. A.; Castellano, F. N.; Meyer, G. J. Enhanced Spectral Sensitivity from Ruthenium(II) Polypyridyl Based Photovoltaic Devices. *Inorg. Chem.* **1994**, *33* (25), 5741−5749.
(23) Deacon, G. B.; Phillips, R. J. Relationships between the carbon-oxygen stretching frequencies of carboxylato complexes and the type of carboxylate coordination. *Coord. Chem. Rev.* **1980**, *33* (3), 227−250.
(24) Heimer, T. A.; D'Arcangelis, S. T.; Farzad, F.; Stipkala, J. M.; Meyer, G. J. An Acetylacetonate-Based Semiconductor−Sensitizer Linkage. *Inorg. Chem.* **1996**, *35* (18), 5319−5324.
(25) Nazeeruddin, M. K.; Liska, P.; Moser, J.; Vlachopoulos, N.; Grätzel, M. Conversion of Light into Electricity with Trinuclear Ruthenium Complexes Adsorbed on Textured TiO2 Films. *Helv. Chim. Acta* **1990**, *73* (6), 1788−1803.
(26) Galoppini, E.; Guo, W.; Zhang, W.; Hoertz, P. G.; Qu, P.; Meyer, G. J. Long-Range Electron Transfer across Molecule−Nanocrystalline Semiconductor Interfaces Using Tripodal Sensitizers. *J. Am. Chem. Soc.* **2002**, *124* (26), 7801−7811.
(27) Wang, Z.-S.; Hara, K.; Dan-oh, Y.; Kasada, C.; Shinpo, A.; Suga, S.; Arakawa, H.; Sugihara, H. Photophysical and (Photo)-electrochemical Properties of a Coumarin Dye. *J. Phys. Chem. B* **2005**, *109* (9), 3907−3914.
(28) Sommeling, P. M.; O'Regan, B. C.; Haswell, R. R.; Smit, H. J. P.; Bakker, N. J.; Smits, J. J. T.; Kroon, J. M.; van Roosmalen, J. A. M. Influence of a TiCl4 Post-Treatment on Nanocrystalline TiO2 Films in Dye-Sensitized Solar Cells. *J. Phys. Chem. B* **2006**, *110* (39), 19191−19197.
(29) O'Regan, B. C.; Durrant, J. R. Kinetic and Energetic Paradigms for Dye-Sensitized Solar Cells: Moving from the Ideal to the Real. *Acc. Chem. Res.* **2009**, *42* (11), 1799−1808.
(30) Keis, K.; Lindgren, J.; Lindquist, S.-E.; Hagfeldt, A. Studies of the Adsorption Process of Ru Complexes in Nanoporous ZnO Electrodes. *Langmuir* **2000**, *16* (10), 4688−4694.
(31) Finklea, H. O. *Semiconductor Electrodes*; Elsevier: Amsterdam, 1988; Vol. *55*.
(32) Ardo, S.; Sun, Y.; Staniszewski, A.; Castellano, F. N.; Meyer, G. J. Stark Effects after Excited-State Interfacial Electron Transfer at Sensitized TiO2 Nanocrystallites. *J. Am. Chem. Soc.* **2010**, *132* (19), 6696−6709.
(33) Cappel, U. B.; Feldt, S. M.; Schöneboom, J.; Hagfeldt, A.; Boschloo, G. The Influence of Local Electric Fields on Photoinduced Absorption in Dye-Sensitized Solar Cells. *J. Am. Chem. Soc.* **2010**, *132* (26), 9096−9101.
(34) Hicks, J. F.; Zamborini, F. P.; Osisek, A. J.; Murray, R. W. The Dynamics of Electron Self-Exchange between Nanoparticles. *J. Am. Chem. Soc.* **2001**, *123* (29), 7048−7053.
(35) Blauch, D. N.; Saveant, J. M. Dynamics of electron hopping in assemblies of redox centers. Percolation and diffusion. *J. Am. Chem. Soc.* **1992**, *114* (9), 3323−3332.
(36) Kelly, C. A.; Farzad, F.; Thompson, D. W.; Stipkala, J. M.; Meyer, G. J. Cation-Controlled Interfacial Charge Injection in Sensitized Nanocrystalline TiO2. *Langmuir* **1999**, *15* (20), 7047−7054.

DOI: 10.1021/acs.langmuir.5b02129
Langmuir 2015, 31, 11164−11178

(37) Watson, D. F.; Meyer, G. J. ELECTRON INJECTION AT DYE-SENSITIZED SEMICONDUCTOR ELECTRODES. *Annu. Rev. Phys. Chem.* **2005**, *56* (1), 119−156.
(38) Higgins, G. T.; Bergeron, B. V.; Hasselmann, G. M.; Farzad, F.; Meyer, G. J. Intermolecular Energy Transfer across Nanocrystalline Semiconductor Surfaces. *J. Phys. Chem. B* **2006**, *110* (6), 2598−2605.
(39) Trammell, S. A.; Yang, J.; Sykora, M.; Fleming, C. N.; Odobel, F.; Meyer, T. J. Molecular Energy Transfer across Oxide Surfaces†. *J. Phys. Chem. B* **2001**, *105* (37), 8895−8904.
(40) Manke, F.; Frost, J. M.; Vaissier, V.; Nelson, J.; Barnes, P. R. F. Influence of a nearby substrate on the reorganization energy of hole exchange between dye molecules. *Phys. Chem. Chem. Phys.* **2015**, *17* (11), 7345−7354.
(41) Hoertz, P. G.; Staniszewski, A.; Marton, A.; Higgins, G. T.; Incarvito, C. D.; Rheingold, A. L.; Meyer, G. J. Toward Exceeding the Shockley−Queisser Limit: Photoinduced Interfacial Charge Transfer Processes that Store Energy in Excess of the Equilibrated Excited State. *J. Am. Chem. Soc.* **2006**, *128* (25), 8234−8245.
(42) Trammell, S. A.; Meyer, T. J. Diffusional Mediation of Surface Electron Transfer on TiO2. *J. Phys. Chem. B* **1998**, *103* (1), 104−107.
(43) Farzad, F. Molecular Level Energy and Electron Transfer Processes at Nanocrystalline Titanium Dioxide Interfaces. Ph.D. Thesis, Johns Hopkins University, 1999.
(44) Wang, Q.; Zakeeruddin, S. M.; Nazeeruddin, M. K.; Humphry-Baker, R.; Grätzel, M. Molecular Wiring of Nanocrystals: NCS-Enhanced Cross-Surface Charge Transfer in Self-Assembled Ru-Complex Monolayer on Mesoscopic Oxide Films. *J. Am. Chem. Soc.* **2006**, *128* (13), 4446−4452.
(45) Li, X.; Nazeeruddin, M. K.; Thelakkat, M.; Barnes, P. R. F.; Vilar, R.; Durrant, J. R. Spectroelectrochemical studies of hole percolation on functionalised nanocrystalline TiO2 films: a comparison of two different ruthenium complexes. *Phys. Chem. Chem. Phys.* **2011**, *13* (4), 1575−1584.
(46) Hu, K.; Robson, K. C. D.; Beauvilliers, E. E.; Schott, E.; Zarate, X.; Arratia-Perez, R.; Berlinguette, C. P.; Meyer, G. J. Intramolecular and Lateral Intermolecular Hole Transfer at the Sensitized TiO2 Interface. *J. Am. Chem. Soc.* **2014**, *136* (3), 1034−1046.
(47) Renault, C.; Balland, V.; Limoges, B.; Costentin, C. Chronoabsorptometry To Investigate Conduction-Band-Mediated Electron Transfer in Mesoporous TiO2 Thin Films. *J. Phys. Chem. C* **2015**, *119* (27), 14929−14937.
(48) Hu, S.; Shaner, M. R.; Beardslee, J. A.; Lichterman, M.; Brunschwig, B. S.; Lewis, N. S. Amorphous TiO2 coatings stabilize Si, GaAs, and GaP photoanodes for efficient water oxidation. *Science* **2014**, *344* (6187), 1005−1009.
(49) Ellmer, K. Past achievements and future challenges in the development of optically transparent electrodes. *Nat. Photonics* **2012**, *6* (12), 809−817.
(50) Boschloo, G.; Fitzmaurice, D. Spectroelectrochemistry of Highly Doped Nanostructured Tin Dioxide Electrodes. *J. Phys. Chem. B* **1999**, *103* (16), 3093−3098.
(51) Frank, S. N.; Bard, A. J. Semiconductor electrodes. II. Electrochemistry at n-type titanium dioxide electrodes in acetonitrile solutions. *J. Am. Chem. Soc.* **1975**, *97* (26), 7427−7433.
(52) Hu, K.; Robson, K. C. D.; Johansson, P. G.; Berlinguette, C. P.; Meyer, G. J. Intramolecular Hole Transfer at Sensitized TiO2 Interfaces. *J. Am. Chem. Soc.* **2012**, *134* (20), 8352−8355.
(53) Ardo, S.; Achey, D.; Morris, A. J.; Abrahamsson, M.; Meyer, G. J. Non-Nernstian Two-Electron Transfer Photocatalysis at Metalloporphyrin-TiO2 Interfaces. *J. Am. Chem. Soc.* **2011**, *133* (41), 16572−16580.
(54) Albery, W. J.; Boutelle, M. G.; Colby, P. J.; Hillman, A. R. The kinetics of electron transfer in the thionine-coated electrode. *J. Electroanal. Chem. Interfacial Electrochem.* **1982**, *133* (1), 135−145.
(55) Chidsey, C. E. D.; Murray, R. W. Redox capacity and direct current electron conductivity in electroactive materials. *J. Phys. Chem.* **1986**, *90* (7), 1479−1484.
(56) Zaban, A.; Ferrere, S.; Gregg, B. A. Relative Energetics at the Semiconductor/Sensitizing Dye/Electrolyte Interface. *J. Phys. Chem. B* **1998**, *102* (2), 452−460.
(57) Hoertz, P. G.; Thompson, D. W.; Friedman, L. A.; Meyer, G. J. Ligand-Localized Electron Trapping at Sensitized Semiconductor Interfaces. *J. Am. Chem. Soc.* **2002**, *124* (33), 9690−9691.
(58) McCord, P.; Bard, A. J. Electrogenerated chemiluminescence: Part 54. Electrogenerated chemiluminescence of ruthenium(II) 4,4′-diphenyl-2,2′-bipyridine and ruthenium(II) 4,7-diphenyl-1,10-phenanthroline systems in aqueous and acetonitrile solutions. *J. Electroanal. Chem. Interfacial Electrochem.* **1991**, *318* (1−2), 91−99.
(59) Gao, F. G.; Bard, A. J. Solid-State Organic Light-Emitting Diodes Based on Tris(2,2′-bipyridine)ruthenium(II) Complexes. *J. Am. Chem. Soc.* **2000**, *122* (30), 7426−7427.
(60) Rudmann, H.; Shimada, S.; Rubner, M. F. Solid-State Light-Emitting Devices Based on the Tris-Chelated Ruthenium(II) Complex. 4. High-Efficiency Light-Emitting Devices Based on Derivatives of the Tris(2,2′-bipyridyl) Ruthenium(II) Complex. *J. Am. Chem. Soc.* **2002**, *124* (17), 4918−4921.
(61) Biancardo, M.; Argazzi, R.; Bignozzi, C. A. Solid-State Photochromic Device Based on Nanocrystalline TiO2 Functionalized with Electron Donor−Acceptor Species. *Inorg. Chem.* **2005**, *44* (26), 9619−9621.
(62) Gardner, J. M.; Beyler, M.; Karnahl, M.; Tschierlei, S.; Ott, S.; Hammarström, L. Light-Driven Electron Transfer between a Photosensitizer and a Proton-Reducing Catalyst Co-adsorbed to NiO. *J. Am. Chem. Soc.* **2012**, *134* (47), 19322−19325.
(63) Ardo, S.; Meyer, G. J. Photodriven heterogeneous charge transfer with transition-metal compounds anchored to TiO2 semiconductor surfaces. *Chem. Soc. Rev.* **2009**, *38* (1), 115−164.
(64) Brigham, E. C.; Achey, D.; Meyer, G. J. Excited state electron transfer from cobalt coordination compounds anchored to TiO2. *Polyhedron* **2014**, *82*, 181−190.
(65) Robson, K. C. D.; Hu, K.; Meyer, G. J.; Berlinguette, C. P. Atomic Level Resolution of Dye Regeneration in the Dye-Sensitized Solar Cell. *J. Am. Chem. Soc.* **2013**, *135* (5), 1961−1971.
(66) Nazeeruddin, M. K.; Humphry-Baker, R.; Liska, P.; Grätzel, M. Investigation of Sensitizer Adsorption and the Influence of Protons on Current and Voltage of a Dye-Sensitized Nanocrystalline TiO2 Solar Cell. *J. Phys. Chem. B* **2003**, *107* (34), 8981−8987.
(67) Concepcion, J. J.; House, R. L.; Papanikolas, J. M.; Meyer, T. J. Chemical approaches to artificial photosynthesis. *Proc. Natl. Acad. Sci. U. S. A.* **2012**, *109* (39), 15560−15564.
(68) Lee, M. M.; Teuscher, J.; Miyasaka, T.; Murakami, T. N.; Snaith, H. J. Efficient Hybrid Solar Cells Based on Meso-Superstructured Organometal Halide Perovskites. *Science* **2012**, *338* (6107), 643−647.
(69) Hagfeldt, A.; Boschloo, G.; Sun, L.; Kloo, L.; Pettersson, H. Dye-Sensitized Solar Cells. *Chem. Rev.* **2010**, *110* (11), 6595−6663.
(70) Song, W.; Ito, A.; Binstead, R. A.; Hanson, K.; Luo, H.; Brennaman, M. K.; Concepcion, J. J.; Meyer, T. J. Accumulation of Multiple Oxidative Equivalents at a Single Site by Cross-Surface Electron Transfer on TiO2. *J. Am. Chem. Soc.* **2013**, *135* (31), 11587−11594.
(71) Swierk, J. R.; McCool, N. S.; Mallouk, T. E. Dynamics of Electron Recombination and Transport in Water-Splitting Dye-Sensitized Photoanodes. *J. Phys. Chem. C* **2015**, *119* (24), 13858−13867.
(72) Holten, D.; Bocian, D. F.; Lindsey, J. S. Probing Electronic Communication in Covalently Linked Multiporphyrin Arrays. A Guide to the Rational Design of Molecular Photonic Devices. *Acc. Chem. Res.* **2002**, *35* (1), 57−69.
(73) Hasselman, G. M.; Watson, D. F.; Stromberg, J. R.; Bocian, D. F.; Holten, D.; Lindsey, J. S.; Meyer, G. J. Theoretical Solar-to-Electrical Energy-Conversion Efficiencies of Perylene−Porphyrin Light-Harvesting Arrays. *J. Phys. Chem. B* **2006**, *110* (50), 25430−25440.
(74) Xu, J.-J.; Zhao, W.-W.; Song, S.; Fan, C.; Chen, H.-Y. Functional nanoprobes for ultrasensitive detection of biomolecules: an update. *Chem. Soc. Rev.* **2014**, *43* (5), 1601−1611.

DOI: 10.1021/acs.langmuir.5b02129
Langmuir 2015, 31, 11164−11178

NOTE ADDED AFTER ASAP PUBLICATION

This article was published ASAP on August 13, 2015, without the required copyright credit lines for Figures 3, 6, and 8−12. The corrected version was reposted on October 2, 2015.

DOI: 10.1021/acs.langmuir.5b02129
Langmuir 2015, 31, 11164−11178